Cathodoluminescence study of the properties of stacking faults in 4*H*-SiC homoepitaxial layers

Serguei I. Maximenko,[1,a)] Jaime A. Freitas, Jr.,[1] Paul B. Klein,[1] Amitesh Shrivastava,[2] and Tangali S. Sudarshan[2]
[1]*Naval Research Laboratory, Washington, D.C. 20375, USA*
[2]*Department of Electrical Engineering, University of South Carolina, Columbia, South Carolina 29208, USA*

(Received 26 November 2008; accepted 9 January 2009; published online 3 March 2009)

In-grown stacking faults in *n*-type 4*H*-SiC epitaxial layers have been investigated by real-color cathodoluminescence imaging and spectroscopy carried out at room and liquid helium temperatures. Stacking faults with 8*H* stacking order were observed, as well as double layer and multilayer 3*C*-SiC structures and a defect with an excitonic band gap at 2.635 eV. It was found that 8*H* stacking faults and triangular surface defects can be generated from similar nucleation sources. Time-resolved measurements reveal that compared to defect-free regions, the carrier lifetimes are severely reduced by the presence of stacking faults corresponding to triangular surface defects and three-dimensional 3*C*-SiC inclusions. © *2009 American Institute of Physics*.
[DOI: 10.1063/1.3089231]

Despite significant improvements in the quality of 4*H*-SiC bulk substrates and epitaxial films during the past decade, there are still a number of crystallographic defects that limit the full development of SiC-based electronic devices. Since high micropipe densities are now commonly avoided and are no longer credited as the most harmful defects for device performance,[1] the elimination of other crystallographic defects, particularly various types of stacking faults (SFs), remains an important issue. This problem becomes more severe as off-cut angles of substrates used for epitaxial growth are decreased from 8° to 4°. These extended defects can result in significant deterioration in the performance and yields of unipolar and bipolar devices.[2,3] While SFs often form as cubic SiC (3*C*-SiC) lamella of variable thicknesses embedded in the 4*H*-SiC host material, 8*H*-like structures have also been reported.[2] SFs can be introduced during film growth (in-grown SFs or IGSFs) or by post-growth processing such as annealing, oxidation, and by mechanical stress. In addition, if Shockley-type basal plane dislocations are present, SFs can develop under carrier injection in the active regions of bipolar devices, or they can be induced by high power laser or e-beam excitation. In spite of their great technological importance and the relatively large amount of work reported in the literature, neither the defect formation mechanisms nor the effect of specific SFs on the electrical properties of epitaxial films is completely understood.

SFs in SiC behave as quantum-well (QW) structures,[4] exhibiting highly efficient radiative recombination due to strong carrier localization in the wells. Consequently, the presence of SFs is easily observed by various luminescence techniques. Due to its unique characteristics, cathodoluminescence (CL) based scanning electron microscopy (SEM) provides the necessary lateral/depth resolution necessary to investigate the optical and electronic properties of SFs.[5] In this work we employ real-color SEM-CL imaging and SEM-CL spectroscopy techniques to detect and identify individual IGSFs. In addition, time-resolved SEM-CL measurements were carried out to determine the effect of IGSFs on the carrier lifetime.

The 4*H*-SiC epitaxial films used in these experiments were typically 18–20 μm thick with *n*-type doping levels of about 7×10^{15} cm^{-3}. The homoepitaxial layers were deposited in a vertical hot-wall inverted chimney chemical vapor deposition (CVD) reactor at a temperature of ~1500 °C using SiH_2Cl_2–C_3H_8–H_2 precursors. Commercially purchased off-cut (0001) 4*H*-SiC wafers oriented 8° toward the $\langle 11\bar{2}0\rangle$ direction were used as substrates. A LEO 435VP SEM fitted with a retractable parabolic light collecting mirror and liquid He cold stage was employed to obtain CL luminescence imaging and CL spectra in the temperature range between 5 and 300 K. The SEM is also equipped with an electrostatic beam blanker, which allows fast time-resolved CL decay measurements. The light emitted by the sample is dispersed by a Triax550 spectrometer fitted with a liquid nitrogen cooled charge-coupled device (CCD) or with a Bialkali photomultiplier for the luminescence decay studies.

Figure 1 shows the room temperature (RT) CL image from a highly defective region, which includes a variety of defects found across the sample. The image was captured with 15 keV accelerating voltage (estimated maximum prob-

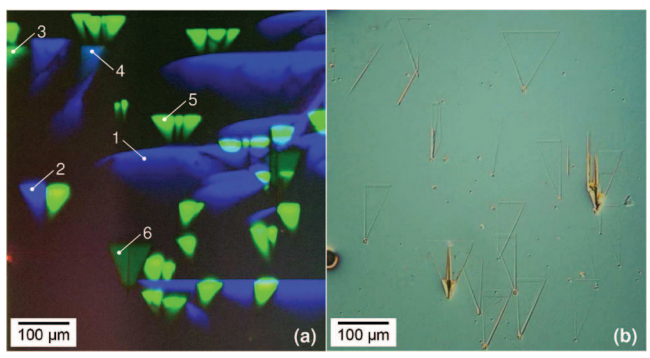

FIG. 1. (Color) (a) RT real-color CL SEM and (b) optical Nomarski images captured from the same part of the sample.

a)Electronic mail: maximenko@bloch.nrl.navy.mil.

ing depth of ~2 μm) (Ref. 6) and 100 nA electron beam current. High excitation level conditions were used to allow the simultaneous observation of defects with high and low radiative efficiencies. Six representative types of defects observed in the sample are marked 1 through 6 in Fig. 1(a) and are distinguished by their characteristic CL spectra. The triangular features of different colors (defects 2–6), with bases aligned parallel to $\langle 1\bar{1}00\rangle$ and apexes pointing toward $\langle 11\bar{2}0\rangle$ direction, are IGSFs commonly observed in SiC epitaxial films,[7] while the defect "1" is a SF induced by the e-beam during the experiments. An optical image [Fig. 1(b)] of the same region, acquired with a Nomarski microscope, reveals that many of SFs observed by CL correspond to well known triangular surface defects (TSDs).[8] The defects marked "1–5" were characterized by a substantial luminescence intensity variation across their lengths, while the defect "6" exhibited a quite uniform intensity distribution. Because the CL intensity is proportional to the concentration of e-h pairs generated and recombining in the probed region, variations in the CL intensity are expected to result from variations in the probed defect depth or thickness.[9] Therefore we can recognize defects 1–5 as thin planar defects embedded within the basal plane (0001) 4*H*-SiC matrix. The fairly uniform CL imaging contrast of defect 6 indicates the presence of a rather three-dimensional (3D) 3*C* inclusion inclined 8° in the basal plane.[10]

The CL spectra, acquired at 5 K and RT, were excited with 15 keV accelerating voltage and 1 nA beam current. The electron beam was aimed at the central part of each selected SF to maximize the density of carriers generated at the SF and prevent luminescence peak shifts resulting from screening introduced by boundary charge accumulation.[5] In addition, the position of the electron beam along the SFs was adjusted so that the maximum in the distribution of generated carriers occurred at the depth of SF, which is approximately 41% of the electron penetration depth.[9] This approach ensures similar injection conditions for all studied defects. The RT CL spectra of the selected SFs exhibited broad emission bands with peaks at 422, 461, 481, 500, and 550 nm, which correspond to the different colors appearing in the real-color CL image depicted in Fig. 1(a). These spectra also include a peak at ~390 nm (3.18 eV), which reflects the near band edge (NBE) emission from the 4*H*-SiC host material. Defects with a blue emission peak at ~422 nm (~2.94 eV, SF1 in Fig. 1) are the common single layer Shockley-type SFs (1SSF) (1,3) generated from basal plane dislocations present in the epitaxial film.[11]

The 5 K CL spectrum of the IGSF "2" (~461 nm; 2.61 eV at RT), represented in Fig. 2(a), shows four well-resolved and relatively sharp peaks at 2.678, 2.647, 2.629, and 2.619 eV. Their energy separations correspond to the TA (~46 meV), LA (~76.6 meV), TO (94.5 meV), and LO (~104.5 meV) phonon replicas associated with the 3*C*-SiC polytype and are considered typical optical signatures of SFs.[12] Using the TA phonon spectral position as a reference, the excitonic band gap (E_{gx}) of this defect was estimated at 2.724 eV. Previous studies correlated this spectrum with a Shockley-type SF of (4, 4) stacking structure, in terms of Zhdanov notation.[2] It was observed that many of the (4, 4) SFs pair with TSDs [defect type "5" in Fig. 1(a)], suggesting that they have common nucleation sites.

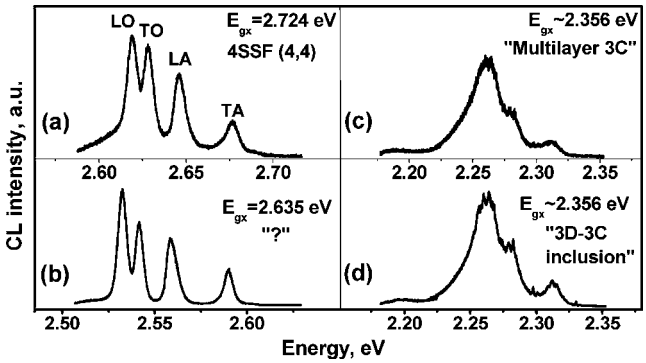

FIG. 2. Low temperature (5 K) CL spectra of some of the defects indicated in Fig. 1: (a) 2, (b) 4, (c) 5, and (d) 6.

The 5 K spectrum of the SF associated with the broad RT CL peak observed at ~500 nm (~2.48 eV) also shows sharp lines assigned to the 3*C*-SiC phonon replicas (not depicted in Fig. 2). The TA phonon energy yields an E_{gx} of 2.506 eV. According to Ref. 13, this excitonic gap is associated with double layer Shockley type SFs [(6,2)SSF]. The observation of this defect in low N-doped samples is unusual since 2SSFs are typically observed in heavily N-doped SiC materials subjected to a high temperature annealing process.[14] The 5 K CL spectrum of defect "4" (broad RT CL band at ~481 nm, ~2.58 eV), shown in Fig. 2(b), also exhibits sharp 3*C*-SiC phonon replicas at low temperature. The energy position of the TA phonon replica of this defect yields an E_{gx} at 2.635 eV. Since higher energy shift of the emission lines of the SFs is expected from lamella with reduced thickness,[15] this defect is expected to have a thickness of less than that of two double layers.

The RT CL band of the IGSFs associated with TSDs and 3D-3*C* inclusions, marked 5 and 6 in Fig. 1(a), respectively, have peaks at ~540 nm (2.29 eV). The low temperature CL spectra of both defects, shown in Figs. 2(c) and 2(d), exhibit broad and poorly resolved phonon replicas. The estimated excitonic gap of these defects is about 2.356 eV, which is below the reported value for bulk 3*C*-SiC (E_{gx}=2.39 eV). The redshift of the phonon replicas for the three 3D-3*C* inclusions, as well as its broadening and intensity quenching, could be related to a high level of incorporated nitrogen impurities and/or to the presence of residual strain.[16,17] The fact that IGSFs associated with surface triangular defects (defect 5 in Fig. 1) have excitonic gaps similar to bulk 3*C*-SiC can be understood from recent computational studies,[15,18] which show that with increasing number of stacked 3*C* layers in a heteropolytype structure 4*H*/QW/4*H*, the SF gap approaches that of the bulk 3*C*-SiC polytype.

The effect of SFs on the carrier lifetime of 4*H*-SiC was probed by the time decay of the RT NBE (~390 nm) emission.[19] The sample was excited with an SEM e-beam pulse width of 50 ns and a repetition rate of 0.1 MHz. An accelerating voltage of 20 keV was employed and current of 40 nA was necessary to produce sufficient signal strength. Under these conditions, the estimated injection level was about $\sim 1.5\times 10^{18}$ cm^{-3}.[20] The effective carrier lifetime (τ_{eff}) was obtained from the exponential decay of the luminescence intensity and reflects contributions from both bulk and surface recombination, $\tau_{\text{eff}}^{-1}=\tau_{\text{bulk}}^{-1}+\tau_{\text{surf}}^{-1}$.

The carrier lifetime in the region near several defects of each type was probed in order to provide reliable results. The

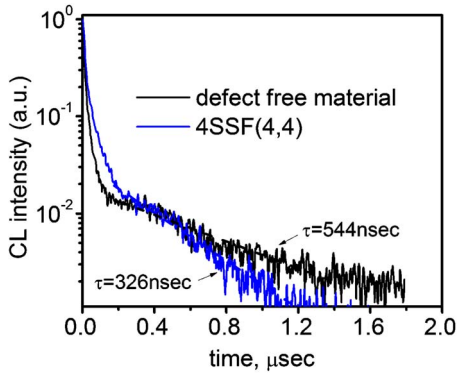

FIG. 3. (Color online) Typical CL decay curves detected from a 4SSF (4,4) defect and from a nearby DFR.

majority of the SFs investigated [(4,4), (6,2), and (E_{gx} =2.356) IGSFs] reflected a very similar influence on the carrier lifetime of the surrounding 4*H*-SiC epitaxial layer. Figure 3 shows a CL decay from a region near these defects compared to a decay from a neighboring defect-free region (DFR). As indicated in Table I, summarizing the lifetime measurements for the various SFs, the lifetime in the DFR was found to be fairly uniform across the sample, in the range of ≈540 ns (but lower at the sample edges, ≈277 ns), while near IGSFs the lifetime was reduced by about 40% to roughly ≈330 ns. Significantly, larger lifetime reductions were observed in regions containing surface triangular defects and 3D-3*C* inclusions. The decay time for one of the double layer IGSFs decreased dramatically, similar to surface triangular defects, which could be explained by the presence of multiple heteropolytype structures aligned in the basal plane.[21]

TABLE I. Summary of time-resolved measurements for different defects. Indicated lifetime errors are ±2 standard deviations.

Defect	Label (Fig. 1)	λ (nm) at RT	E_{gx} (eV) at 5 K	τ_{eff} (ns) DFR	τ_{eff} (ns) at SF
4SSF(4,4)	2	461	2.724	544 ± 28	326 ± 24
2SSF(6,2)	3	500	2.506	548 ± 24	330 ± 30
?	4	481	2.635	537 ± 26	339 ± 26
TSD[b]	5	540	2.356	277 ± 24	15 ± 5 [a]
3D-3*C* incl.[b,c]	6	540	2.356	277 ± 25	15 ± 5 [a]

[a]Value close to the experimental resolution limit.
[b]Measured close to the sample edge.
[c]Found only about sample edges.

In summary, it was demonstrated that real-color CL imaging provides a quick and nondestructive identification of several different types of SFs with high spatial resolution. CL spectra of several distinct SF structures have been determined. Time-resolved CL measurements show shorter lifetimes near IGSFs and that SFs corresponding to TSDs and 3D-3*C* inclusions strongly reduce the carrier lifetime in the region near these SFs. Multiple-layer SF structures appear to also have a strong influence on the carrier lifetime.

The research at NRL was partially supported by the Office of Naval Research. S.I.M. thanks the NRC program at NRL for support.

[1]R. T. Leonard, Y. Khlebnikov, A. R. Powell, C. Basceri, M. F. Brady, I. Khlebnikov, J. R. Jenny, D. P. Malta, M. J. Paisley, V. F. Tsvetkov, R. Zilli, E. Deyneka, H. Hobgood, V. Balakrishna, and C. H. Carter, Jr., Mater. Sci. Forum **600**, 7 (2009).
[2]H. Fujiwara, T. Kimoto, T. Tojo, and H. Matsunami, Appl. Phys. Lett. **87**, 051912 (2005).
[3]H. Lendenmann, F. Dahlquist, N. Johansson, R. Söderholm, J. Per Åke Nilsson, P. Bergman, and P. Skytt, Mater. Sci. Forum **353**, 727 (2001).
[4]H. Iwata, U. Lindefelt, S. Öberg, and P. R. Briddon, Phys. Rev. B **65**, 033203 (2001).
[5]S. Juillaguet, M. Albrecht, J. Camassel, and T. Chassagne, Phys. Status Solidi A **204**, 2222 (2007).
[6]K. Kanaya and S. Okayama, J. Phys. D **5**, 43 (1972).
[7]G. Feng, J. Suda, and T. Kimoto, Appl. Phys. Lett. **92**, 221906 (2008).
[8]T. Okada, T. Kimoto, K. Yamai, H. Matsunami, and F. Inoko, Mater. Sci. Eng., A **361**, 67 (2003).
[9]B. G. Yacobi and D. B. Holt, *Cathodoluminescence Microscopy of Inorganic Solids*, 1st ed. (Springer, New York, 1990), p. 65.
[10]A. Shrivastava, P. Muzykov, J. D. Caldwell, and T. S. Sudarshan, J. Cryst. Growth **310**, 4443 (2008).
[11]A. Galeckas, A. Hallen, S. Majdi, J. Linnros, and P. Pirouz, Phys. Rev. B **74**, 233203 (2006).
[12]S. Bai, R. P. Devaty, W. J. Choyke, U. Kaiser, G. Wagner, and M. F. MacMillan, Appl. Phys. Lett. **83**, 3171 (2003).
[13]K. Irmscher, J. Doerschel, H.-J. Rost, D. Schulz, D. Siche, M. Nerding, and H. P. Strunk, Eur. Phys. J.: Appl. Phys. **27**, 243 (2004).
[14]J. Q. Liu, H. J. Chung, T. Kuhr, Q. Li, and M. Skowronski, Appl. Phys. Lett. **80**, 2111 (2002).
[15]J. Camassel and S. Juillaguet, J. Phys. D **40**, 6264 (2007).
[16]A. Henry, U. Forsberg, M. K. Linnarsson, and E. Janzén, Phys. Scr. **72**, 254 (2005).
[17]W. J. Choyke, Z. C. Feng, and J. A. Powell, J. Appl. Phys. **64**, 3163 (1988).
[18]M. S. Miao and W. R. L. Lambrecht, J. Appl. Phys. **101**, 103711 (2007).
[19]J. P. Bergman, O. Kordina, and E. Janzén, Phys. Status Solidi A **162**, 65 (1997).
[20]D. K. Schroder, *Semiconductor Material and Device Characterization*, 2nd ed. (Wiley, New York, 1998).
[21]J. D. Caldwell, P. B. Klein, M. E. Twigg, R. E. Stahlbush, O. J. Glembocki, K. X. Liu, K. D. Hobart, and F. Kub, Appl. Phys. Lett. **89**, 103519 (2006).